THE JOURNAL OF BIOLOGICAL CHEMISTRY
Vol. 275, No. 39, Issue of September 29, pp. 30690–30700, 2000

Printed in U.S.A.

Cloning of the cDNAs Coding for Two Novel Molybdo-flavoproteins Showing High Similarity with Aldehyde Oxidase and Xanthine Oxidoreductase*

Received for publication, June 20, 2000, and in revised form, July 7, 2000
Published, JBC Papers in Press, July 11, 2000, DOI 10.1074/jbc.M005355200

Mineko Terao, Mami Kurosaki, Giuliana Saltini, Silvia Demontis, Massimiliano Marini, Mario Salmona, and Enrico Garattini‡

From the Laboratory of Molecular Biology, Centro Catullo e Daniela Borgomainerio, Istituto di Ricerche Farmacologiche "Mario Negri," via Eritrea, 62, 20157 Milano, Italy

The cDNAs coding for two novel mouse molybdo-flavoproteins, AOH1 and AOH2 (aldehyde oxidase homolog 1 and 2), were isolated. The AOH1 and AOH2 cDNAs code for polypeptides of 1336 amino acids. The two proteins have similar primary structure and show striking amino acid identity with aldehyde oxidase and xanthine oxidoreductase, two other molybdo-flavoenzymes. AOH1 and AOH2 contain consensus sequences for a molybdopterin-binding site and two distinct 2Fe-2S redox centers. In its native conformation, AOH1 has a molecular weight consistent with a homotetrameric structure. Transfection of the AOH1 and AOH2 cDNAs results in the production of proteins with phenanthridine but not hypoxanthine oxidizing activity. Furthermore, the AOH1 protein has benzaldehyde oxidizing activity with electrophoretic characteristics identical to those of a previously identified aldehyde oxidase isoenzyme (Holmes, R. S. (1979) *Biochem. Genet.* 17, 517–528). The AOH1 transcript is expressed in the hepatocytes of the adult and fetal liver and in spermatogonia. In liver, the AOH1 protein is synthesized in a gender-specific fashion. The expression of AOH2 is limited to keratinized epithelia and the basal layer of the epidermis and hair folliculi. The selective cell and tissue distribution of AOH1 and AOH2 mRNAs is consistent with the localization of the respective protein products.

Molybdo-proteins are enzymes that require a molybdopterin cofactor (molybdenum cofactor) for their catalytic activity (1). These proteins are widely distributed in nature being present in bacteria (2), yeasts (3), plants (4, 5) insects, and vertebrates (1, 6). In mammals, three molybdo-proteins have been identified and characterized, *i.e.* sulfite oxidase (7), xanthine oxidoreductase (XOR),[1] (8–12) and aldehyde oxidase (AO) (13–16). Unlike sulfite oxidase, XOR and AO utilize a flavin besides the molybdenum cofactor to oxidize their respective substrates (8–16). Thus, the two proteins are the only known members of the subfamily of mammalian molybdo-flavoenzymes.

XOR and AO have a striking number of similarities. They act on a partially overlapping set of substrates, which include *N*-heterocyclic compounds (17), have a high level of amino acid identity (1), as well as similar molecular weights and secondary/tertiary structure (18, 19). In addition, the corresponding genes have a common origin, as recently indicated by the high degree of conservation of the exon/intron junctions (20–22). XOR is the key enzyme in the catabolism of purines oxidizing hypoxanthine to xanthine and xanthine to uric acid, although the physiological function of this protein may be more complex than anticipated (23, 24). Because of its ability to produce toxic superoxide anions, the oxidase form of XOR (25) has been implicated as a possible mediator of tissue damage in a number of pathological situations, such as ischemia (26), inflammation (27), and infection (28). AO is much less studied, and a physiological substrate for the enzyme has not yet been established, although there are reports indicating that the enzyme oxidizes retinaldehyde into retinoic acid (29) and is involved in the catabolism of the monoamine neurotransmitters (30). Moreover, the AO protein is of considerable pharmacological and toxicological importance, given its role in the metabolism of drugs such as methotrexate (31) and cyclophosphamide (32). Finally, the *AO* gene has been recently implicated in the etiopathogenesis of the familial recessive form of amyotrophic lateral sclerosis, a rare motor neuron disease (33).

In plants, distinct AO isoenzymes have been described (4, 5, 34). Similarly, in the animal kingdom, the family of molybdo-flavoproteins may extend beyond AO and XOR. Wright and Repine (35) postulated the presence of multiple AO variants in humans, and Holmes (36) reported on the existence of two benzaldehyde oxidase enzymatic activities with different electrophoretic characteristics in mouse liver. The two enzymatic variants are the products of separate genes, named *AOX1* and *AOX2,* and mapped on chromosome 1 by classical genetic analysis (36). In a previous article (22), we isolated the murine *AO* gene and suggested that it is identical to *AOX2*. In this report, we describe the identification and structural characterization of two novel mouse cDNAs coding for putative molybdo-flavoproteins, which we named AOH1 and AOH2 (aldehyde oxidase homolog 1 and 2) because of the enzymatic characteristics and the high level of similarity with AO. We demonstrate that

* This work was supported in part by grants from the Telethon-Italy Grant 88 (to M. T.), from the Associazione per la Ricerca Contro il Cancro, from the Consiglio Nazionale delle Ricerche, Progetto Finalizzato Biotecnologie, and from the MURST. The costs of publication of this article were defrayed in part by the payment of page charges. This article must therefore be hereby marked "*advertisement*" in accordance with 18 U.S.C. Section 1734 solely to indicate this fact.

The nucleotide sequence(s) reported in this paper has been submitted to the GenBank™/EBI Data Bank with accession number(s) AF172276 and AF233581.

‡ To whom correspondence should be addressed. Tel.: 39-02-39014533; Fax: 39-02-3546277; E-mail: egarattini@irfmn.mnegri.it.

[1] The abbreviations used are: XOR, xanthine oxidoreductase; AOH1, aldehyde oxidase homolog 1; AOH2, aldehyde oxidase homolog 2; AO = aldehyde oxidase; RACE, rapid amplification of cDNA ends; kb, kilobase pair; aa, amino acid; PCR, polymerase chain reaction; PAGE, polyacrylamide gel electrophoresis; MTT, 3-(4,5-dimethylthiazol-2-yl)-2,5-diphenyl tetrazolium bromide; FPLC, fast protein liquid chromatography; PMS, *N*-methylphenazonium methyl sulfate; DgAOx, *D. gigas* aldehyde oxidoreductase.

AOH1 is the product of the *AOX1* gene and confirm that AO is encoded by the *AOX2* locus.

EXPERIMENTAL PROCEDURES

Molecular Cloning and Sequencing of the cDNAs Encoding AOH1 and AOH2—The mouse ESTs AA64385 and AA79991 were obtained from the UK Human Genome Mapping Project Resource Center (Cambridge, UK). To obtain the full-length nucleotide sequence of the AOH1 cDNA, a mouse liver library (CLONTECH, Palo Alto, CA) was screened with AA64385 as a probe according to standard protocols (37). This resulted in the isolation of 40 hybridizing clones that were categorized according to their pattern of digestion with several restriction enzymes. Three lambda clones (24/1, 62/1, and 123/1) overlapping with AA64385 and covering the 5′ and 3′ portions of the AOH1 transcript were subcloned in pBluescript (Stratagene, La Jolla, CA) and further characterized. The missing 5′ portion of the AA79991 cDNA was obtained by nested 5′-RACE from mouse skin poly(A^+) RNA, using a commercially available kit (CLONTECH). The two antisense oligonucleotides used for the primary and nested amplifications were 5′-AGTTTGTGGGATAGCCAGGATGGT-3′ (complementary to nucleotide 2368–2391 of the AOH2 sequence) and 5′-TGTAAAAGTGTTCCTGCCCTTCCACG-3′ (complementary to nucleotide 2331–2356), respectively. The resulting 2.3-kb-long fragment was subcloned in pBluescript (AOH2 5′-RACE). The continuity of clones AA79991 and AOH2–5′-RACE was confirmed by further PCR amplification experiments resulting in the synthesis of clones AOH2-PCR1 and AOH2-PCR2. Nucleotide sequencing was performed according to the dideoxy chain termination method (38), using T7-DNA polymerase (Amersham Pharmacia Biotech). All the cDNAs were sequenced in both directions using either T7 and T3 or sequence-specific oligonucleotides, which were custom-synthesized by Europrime (Life Technologies, Inc.).

Reconstruction of the Full-length AOH1 and AOH2 cDNAs and Expression in Eukaryotic Cells—For the reconstruction of the full-length AOH1 cDNA, two DNA fragments, *Cla*I-*Stu*I (fragment a, containing nucleotide 1–2093) and *Stu*I-*Eco*RI (fragment b, nucleotide 2094–3929), were obtained from the pBluescript sub-clones 24/1 and 62/1, respectively. The 3′ portion of the AOH1 coding sequence was amplified by reverse transcriptase-PCR from liver poly(A^+) RNA using the two amplimers, 5′-CACCTGAAGGAGTCCTATACACTC-3′ (nucleotide 3858–3881) and 5′-atgcggccggGCTGGAACCCCAAGCACTAG-3′ (complementary to nucleotide 4207–4226; the lowercase letters represent the sequence of an artificial *Not*I site introduced to facilitate cloning). The resulting fragment was digested with *Eco*RI and *Not*I (fragment c, nucleotide 3930–4226). The entire coding sequence of AOH1 was obtained by introducing fragments, a–c, into the *Not*I site of pBluescript (AOH1-pBluescript). To express the AOH1 protein in eukaryotic cells, the corresponding complete coding sequence was amplified from AOH1-pBluescript by long range PCR using rTth DNA polymerase (Perkin-Elmer) and the two amplimers, 5′-ttgcggccgctcgaaggagatagaaccATGTCTCCTTCTAAGGAGTCAGATGAGC-5′ (nucleotide 200–227; the lowercase letters represent an artificial *Not*I site and an artificial ribosomal binding sequence) and 5′-ttgcggccgccCTAGGCAACTGGGATGGACCACGGCTTA-3′ (complementary to nucleotide 4183–4210; the lowercase letters represent an artificial *Not*I site). The amplified 4-kb fragment was digested with *Not*I and inserted downstream of the promoter region of the plasmid pCMVβ (CLONTECH) previously digested with *Not*I to eliminate the β-galactosidase gene. The orientation of the insert was determined by restriction digest and confirmed by sequence analysis.

To reconstruct the full-length AOH2 cDNA, the clone 5′-RACE containing the 5′ portion of the cDNA was digested with *Not*I and *Eco*RI (fragment d, nucleotide 1–946). The middle part of the cDNA was amplified by reverse transcriptase-PCR from liver poly(A^+) RNA using two amplimers, 5′-GTCATGGGGAACACCACAGT-3′ (nucleotide 901–920) and 5′-CATCTTAGTGTGTAGGCCTTGTCC-3′ (complementary to nucleotide 3241–3264). The resulting fragment was digested with *Eco*RI and *Stu*I (fragment e, nucleotide 947–3248). To obtain AOH2-pBluescript, fragments d and e were inserted in the clone AA79991, which was previously digested with *Not*I and *Stu*I. The strategy used to introduce the coding sequence of AOH2 into the pCMV vector was essentially the same as for AOH1. The clone AOH2-pBluescript was used as a template for long range PCR with the following amplimers: 5′-ttgcggccgctcgaaggagctagaaccATGCCTTCCGTCTCCGAGTCTGACGAGC-3′ (nucleotide 106–133) and 5′-ttgcggccgccTTAAGACACGTGGATGGACCAAGGTGTG-3′ (complementary to nucleotide 4089–4116). The amplified 4-kb fragment was digested with *Not*I and inserted downstream of the promoter region of the plasmid pCMVβ.

Transfection of the AOH1 and AOH2 cDNAs—The HEK293 human embryonic kidney fibroblastic cell line, obtained from ATCC, was maintained in Dulbecco's modified Eagle's medium containing 10% fetal calf serum, and the HC11 mouse mammary epithelial cell line, a kind gift of Dr. Nancy Hynes (FMI, Basel Switzerland), was routinely passaged in RPMI 1640 containing 10% fetal calf serum, 5 μg/ml insulin (Sigma), and 10 ng/ml epidermal growth factor (Sigma). The full-length mouse AOH1 and AOH2 cDNAs cloned in pCMVβ (AOH1-pCMV and AOH2-pCMV) were transfected into the HEK293 and HC11 cell lines using LipofectAMINE (Life Technologies, Inc.), according to the instructions of the manufacturer. Forty eight hours following transfection, cell extracts were analyzed for their oxidizing activity using benzaldehyde (39) and phenanthridine (40) as substrates and for the presence of the respective protein products by Western blot analysis as described in the following sections.

Enzymatic Activity Measurements—Mouse tissues were homogenized in 50 mM potassium phosphate buffer (pH 7.4) containing EDTA (0.1 mM), phenylmethylsulfonyl fluoride (0.1 mM), leupeptin (2 μM), and aprotinin (0.15 μM) and ultracentrifuged at 105,000 $\times$ *g* for 1 h. The supernatant was used to determine benzaldehyde-oxidizing activity. The extracts of cells transfected with the AOH1, AOH2, and AO cDNAs were lysed by freezing/thawing in the homogenization buffer containing 0.1% Triton X-100.

Phenanthridine-oxidizing activity was measured spectrophotometrically as described by Taylor *et al.* (40). One unit of enzyme activity is defined as 1 μmol of 6-phenanthridone (ϵ = 10,000 at 322 nm) produced per min. Benzaldehyde or hypoxanthine oxidizing activity was determined following electrophoresis on cellulose acetate plates (TITAN III, Helena Laboratories, Beaumont, TX) and staining with the appropriate substrate, as described by Holmes (36, 39). Briefly, plates were run at 200 V for 20 min in 25 mM Tris, 192 mM glycine buffer and stained by overlaying 6% agarose gel containing 100 mM Tris (pH 8.0), 25 mM benzaldehyde or hypoxanthine, 0.9 mM 3-(4,5-dimethylthiazol-2-yl)-2,5-diphenyl tetrazolium bromide (MTT), and 0.3 mM *N*-methylphenazonium methyl sulfate (PMS) (39). Proteins were measured according to the Bradford method using a commercially available kit (Bio-Rad).

Western Blot Analysis—The anti-AOH1, anti-AOH2, and anti-AO polyclonal sera were obtained from rabbits immunized with the following synthetic peptides covalently attached to polylysine according to the multiple antigenic peptide technology (41): H-Gln-Phe-Thr-Asn-Leu-Val-Pro-Gln-Thr-Asp-Ser-Lys-OH (aa 1315–1326 of AOH1), H-Thr-His-Val-Gln-Glu-Phe-Val-Ser-Ala-Ala-Leu-Asn-Val-Pro-Arg-Ser-Arg-Ile-Ala-OH (aa 777–795 of AOH2), and H-Thr-Glu-Met-His-Ile-Ser-Phe-Leu-Pro-Pro-Ser-Glu-His-Ser-Asn-Thr-Leu-Lys-OH (aa 1241–1258 of mouse AO; 14).

Sodium dodecyl sulfate-polyacrylamide gel electrophoresis (PAGE) was performed under reducing conditions according to the standard protocol of Laemmli following preparation of samples as described below. Mouse tissues were homogenized and ultracentrifuged as described above. The cytosolic supernatants were heated at 55 °C for 10 min and briefly centrifuged to eliminate the protein precipitate. The resulting supernatants were analyzed by SDS-PAGE. Extracts of cells transfected with the mouse AOH1, AOH2, and AO cDNAs were lysed by sonication and centrifuged at 10,000 $\times$ *g* for 5 min at 4 °C prior to SDS-PAGE. Following electrophoresis on 6.0% gels, proteins were electrotransferred onto nitrocellulose membranes (Schleicher & Schuell). Membranes were incubated with optimal dilutions of primary antibodies (1–3,000 for anti-AOH1 serum and 1–1,000 for anti-AOH2 and anti-AO sera) and a 1–2,500 dilution of goat anti-rabbit IgG secondary antibody linked to horseradish peroxidase (Sigma). Specific AOH1, AOH2, and AO bands were visualized by autoradiography on X-Omat films (Eastman Kodak Co.), using a commercially available kit (ECL, Amersham Pharmacia Biotech) based on a peroxidase-specific chemiluminescent substrate.

Partial Purification of Mouse Liver AOH1 and Column Chromatography—The AOH1 protein was partially purified from mouse liver by benzamidine-Sepharose affinity chromatography (Amersham Pharmacia Biotech) exactly as described for bovine AO (13). Following elution with benzamidine (Sigma), active fractions were concentrated by ultrafiltration on Centricon YM-100 cartridges (Millipore, Bedford, MA) and applied to a gel filtration FPLC Superose-6 column (Amersham Pharmacia Biotech) run at 0.5 ml/min in phosphate-buffered saline (pH 7.4), containing 100 mM NaCl. Fractions of 0.5 ml were collected, and aliquots thereof were analyzed for benzaldehyde-oxidizing activity by electrophoresis on cellulose acetate plates or AOH1 and AO immunoreactivity by Western blot analysis.

Northern Blot Analysis and in Situ Hybridization—Northern blot analysis was performed as described previously (8), using total RNA or

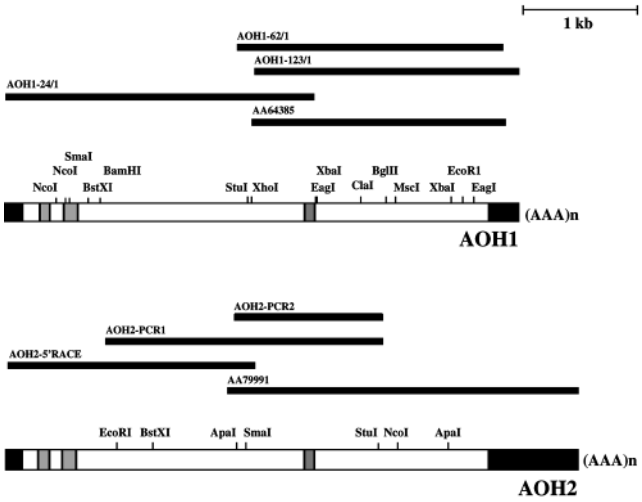

FIG. 1. **Structural organization and physical map of mouse liver AOH1 and mouse skin AOH2 cDNAs.** The figure represents the physical map of mouse liver AOH1 and mouse skin AOH2 cDNAs from the 5′- to the 3′-end (*left* to *right*). The 5′- and 3′-untranslated regions of the two cDNAs are indicated by *black boxes*, and the coding sequences are indicated by *white boxes. Dotted boxes* and *dashed boxes* represent the 2Fe-2S redox centers and the molybdo-protein fingerprint sequences, respectively. Sites for selected restriction endonucleases are indicated. The poly(A^+) tail is indicated by (*AAA*)*n*. The *thick lines* represent inserts of the original EST clones (AA64385 and AA79991), secondary recombinant lambda phages, and PCR products. All the clones were sequenced completely in both directions.

poly(A^+) RNA and ^{32}P-radiolabeled AOH1 and AOH2 or glyceraldehyde-3-phosphate dehydrogenase (42) cDNAs as probes.

The *Xho*I-*Xba*I fragment of AOH1 cDNA (nucleotides 2131–2696) and a PCR-amplified fragment of AOH2 cDNA (nucleotides 4169–4787) were subcloned in pBluescript and used as templates for the synthesis of sense and antisense riboprobes, employing T3 and T7 RNA polymerases (Stratagene), in the presence of [^{35}S]thio-UTP (specific radioactivity 1200 Ci/mmol, Amersham Pharmacia Biotech). Template DNAs were degraded by DNase I (Amersham Pharmacia Biotech), and the average length of the riboprobes was adjusted to approximately 150 nucleotides by alkaline treatment (43). Mouse tissues were fixed in 4% paraformaldehyde overnight, embedded in paraffin, sectioned to 5-μm thickness, and mounted on chromalum-containing gelatin-coated slides. The conditions for the pretreatment of slides, hybridization, washing, and detection by the nuclear track emulsion technique were precisely as described in a previous report (23). At the end of the *in situ* hybridization procedure, tissue sections were stained with hematoxylin-eosin and photographed under the microscope.

RESULTS

Molecular Cloning of the AOH1 and AOH2 cDNAs—Screening of the mouse dbEST section of GenBank™ for sequences showing similarity with murine AO and XOR resulted in the identification of two distinct ESTs (AA64385 and AA79991) derived from testis and skin, respectively. Northern blot experiments conducted with the AA64385 and the AA79991 clones indicated that the two cDNAs were incomplete copies of larger transcripts. To isolate the full-length cDNAs we used different strategies. As to AA64385, screening of a mouse liver cDNA library resulted in the isolation of overlapping clones and the determination of the entire primary structure of a cDNA, which we named AOH1 (aldehyde oxidase homolog 1). As to the second EST, the missing portion of the cDNA corresponding to clone AA79991 was obtained by 5′-RACE using RNA isolated from mouse skin. This second full-length cDNA was named AOH2 (aldehyde oxidase homolog 2). A summary of the cloning results is shown in Fig. 1.

As shown by Figs. 2 and 3, the longest open reading frames of both the AOH1 and AOH2 cDNAs are exactly the same length and predict two distinct polypeptides of 1336 amino acids. The 5′-untranslated regions of AOH1 and AOH2 are 199 and 105 nucleotides long, respectively, and they do not contain any in-frame ATG triplet upstream of the the putative first Met codon. The 3′-untranslated regions of AOH1 and AOH2 are 222 and 780 nucleotides long, respectively, and they both terminate with a polyadenylated tail preceded by canonical polyadenylation signals. The AOH1 and AOH2 polypeptides are very likely to code for molybdoenzymes, as they both contain a slight variant of the typical fingerprint sequence (aa 802–837 of AOH1 and aa 804–839 of AOH2) found in all the members of this class of proteins (44). In AOH1 and AOH2, the only amino acid differing from the canonical molybdo-protein consensus sequence present in the PROSITE data base (44) is a phenylalanine (Phe-830) which takes the place of a generally conserved cysteine residue. This is not unprecedented, since this cysteine is also substituted by hydrophobic amino acids in *Arabidopsis thaliana* AO (34), *Drosophila melanogaster* XOR (45), and *Bombyx mori* XOR (46).

Similarity of AOH1 and AOH2 Proteins to AOs and XORs—The primary structure of both AOH1 and AOH2 proteins has a significant level of similarity with XORs and AOs of various origin, as demonstrated by the phylogenetic tree shown in Fig. 4. This indicates that the two novel enzymes belong to the family of molybdo-flavoproteins. AOH1 and AOH2 are most similar to each other (63% amino acid identity) and constitute a distinct structural subgroup within the mammalian aldehyde oxidase cluster, which, in turn, is clearly separated from the XOR subfamily. Like mammalian AOs, mouse AOH1 and AOH2 are more related to animal XORs than to plant AOs.

As illustrated in Fig. 5, the amino acid sequences of AOH1 and AOH2 can be aligned along their entire length with mouse AO and XOR (14, 8). AOH1 and AOH2 show an overall identity of 60 and 58% with mouse AO and 50 and 47% with mouse XOR, respectively. A search in the PROSITE data bank indicates that both AOH1 and AOH2 have a sequence (aa 116–159) similar to that of the ferredoxin-type 2Fe/2S redox centers (44) highly conserved in all the AO and XOR proteins (3–5, 8–10, 12–14, 34, 45–49). This is preceded by another stretch of amino acids (aa 47–78), which is very similar to that of the second 2Fe/2S redox center also present in all molybdo-flavoenzymes. Notably, the position of the 8 cysteine residues (aa 47, 52, 55, 77, 117, 120, 152, and 154) involved in the coordination of the iron ions in the two redox centers of the AO and XOR proteins is strictly conserved in AOH1 and AOH2. AOH1 and AOH2 lack the FAD-binding signature sequence described by Correll *et al.* (51) in various types of flavoproteins, which, however, is not found in AOs and XORs.

Desulfovibrio gigas aldehyde oxidoreductase (DgAOX; Ref. 52) is the only molybdo-protein showing similarity with XOR and AO, for which crystallographic data are available (53). In DgAOX, the molybdenum site has been divided into 5 domains (MoCoI–MoCoV). The GGTFGYK sequence of the MoCoI site of DgAOX (aa 418–424) is very well conserved in both AOH1 (aa 800–806) and AOH2 (aa 802–808). A high degree of amino acid identity among AOH1, AOH2, AO, XOR, and DgAOX is also observed in the sequences corresponding to the MoCoII (aa 915–923 of AOH1 and aa 917–925 of AOH2) and MoCoIII (aa 1043–1046 of AOH1 and aa 1045–1048 of AOH2) sites of the prokaryotic aldehyde oxidoreductase (AFRGYGAPQSM; aa 531–541; HGQG; aa 653–656). By contrast, the level of amino acid conservation in the sequences of AOH1 and AOH2 corresponding to the MoCoIV (GPSGGS; aa 693–698) and MoCoV (VGELPL; aa 867–872) of DgAOX is low. In DgAOX, the molybdenum site is buried in the center of the protein, and it is accessible through a tunnel that is coated by 20 hydophobic residues (53). Some of these amino acids have conserved counterparts not only in AOH1 (Gly-804, Ala-915, Phe-919, Phe-

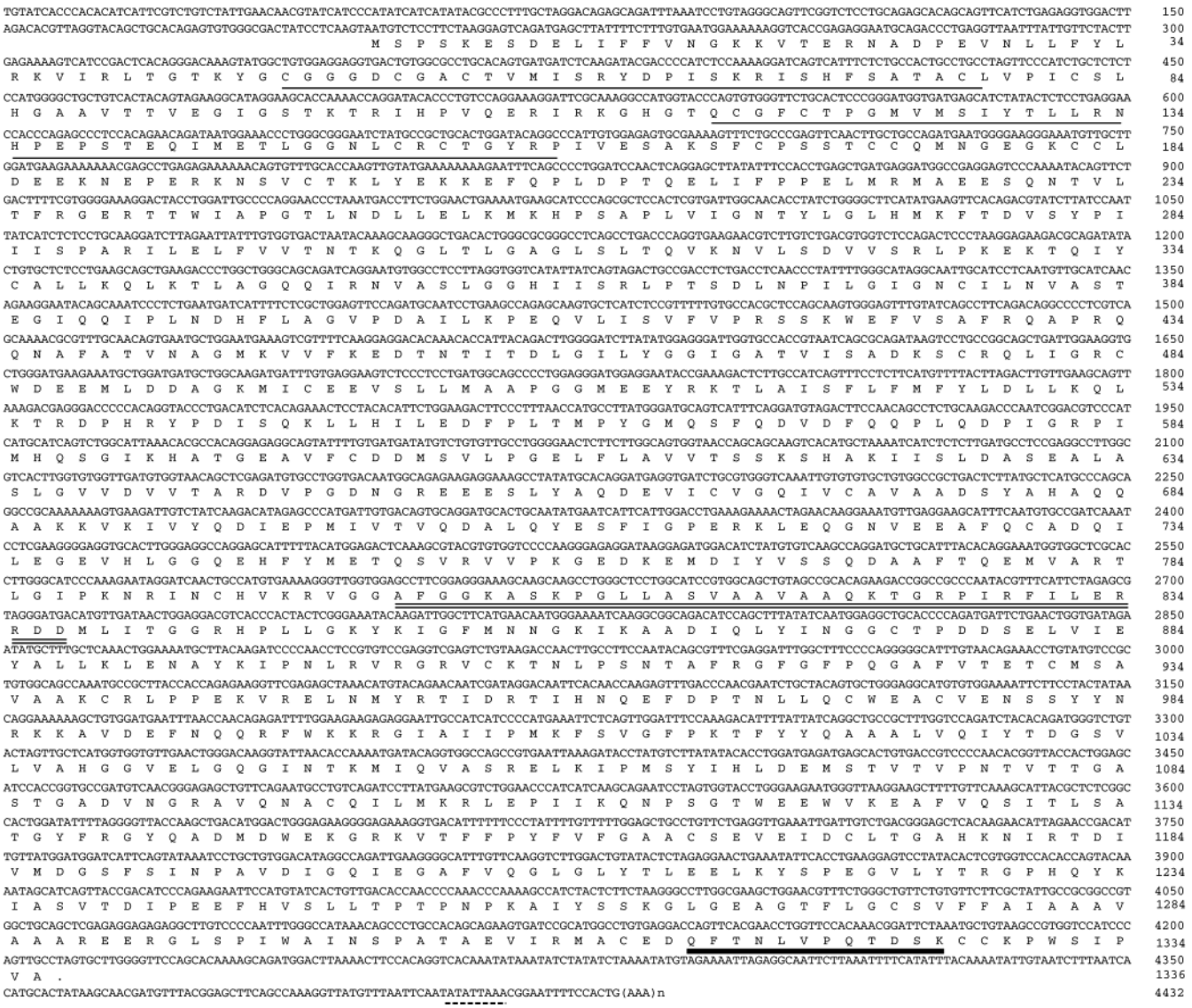

FIG. 2. **Nucleotide and deduced amino acid sequence of mouse liver AOH1.** The nucleotide sequence of the AOH1 cDNA (*upper line*) was obtained from the overlapping cDNA fragments shown in Fig. 1 and is presented with its deduced amino acid sequence (*lower line*). Nucleotides are numbered in the 5′–3′ direction, whereas amino acids are numbered from the amino terminus to the carboxyl terminus starting from the putative first methionine residue. (*AAA*)*n* indicates the polyadenylated tail of the transcript. The sequences corresponding to the 2Fe-2S redox centers are *underlined*, and the molybdo-protein fingerprint sequence is *doubly underlined*. The *dotted line* indicates the polyadenylation signal. The *thick line* indicates the peptide used to raise specific anti-AOH1 polyclonal antibodies.

1010, Phe-1014, Asn-1078, and Ala-1084) and AOH2 (Gly-806, Ala-917, Phe-921, Phe-1012, Val-1016, Asn-1080, and Gly-1086) but also in mouse AO and XOR.

As observed in the case of mammalian AOs, the regions of AOH1 and AOH2 equivalent to the substrate binding pocket defined for DgAOX (53) contain a hydrophobic amino acid (Ala-807 in AOH1 and Val-809 in AOH2) in the same position in which a conserved Glu residue is present in XORs (aa 805 in the mouse enzyme). In addition, the mouse XOR Arg-883 residue, which is maintained in all XOR proteins and altered in *Aspergillus nidulans* mutants unable to utilize 2-hydroxypurines (54), is changed into a hydrophobic Tyr (position 885), Phe (position 887), or Met (position 884) in AOH1, AOH2 and AO, respectively. As these amino acids seem to be important for the substrate specificity of XORs (1, 53), it is conceivable that AOH1 and AOH2 do not use hypoxanthine or xanthine as substrates. Interestingly, like AO, neither AOH1 nor AOH2 contain the sequence FFPGYRR (positions 391–397 of mouse XOR) responsible for the binding of NAD in chicken xanthine dehydrogenase (55) and conserved in all the XORs of animal origin (8–10, 12, 47). All this suggests that AOH1 and AOH2 are not only structurally but also biochemically more related to AO than to XOR.

Structural and Enzymatic Characteristics of the AOH1 and AOH2 Proteins—To gain further information on the two novel proteins, we first developed antibodies specific for AOH1, AOH2, and AO. For this purpose, we immunized rabbits with polypeptides corresponding to regions of low similarity among the three proteins. The specificity of these reagents was tested using extracts from HEK293 cells transfected with the cDNAs coding for AOH1 (pCMV-AOH1), AOH2 (pCMV-AOH2), and AO (pCMV-AO). As shown in Fig. 6*A*, the anti-AOH1 antibody recognizes a single band of approximately 150 kDa in extracts of cells programmed to synthesize the AOH1 protein but not in extracts transfected with pCMV-AOH2, pCMV-AO, or the corresponding empty vector (pCMV). Similarly, the anti-AOH2 and anti-AO antibodies highlight a specific 150-kDa protein band only in cells forced to express the corresponding proteins. The apparent molecular weight of the bands observed in extracts of cells transfected with the AOH1 and AOH2 cDNAs is

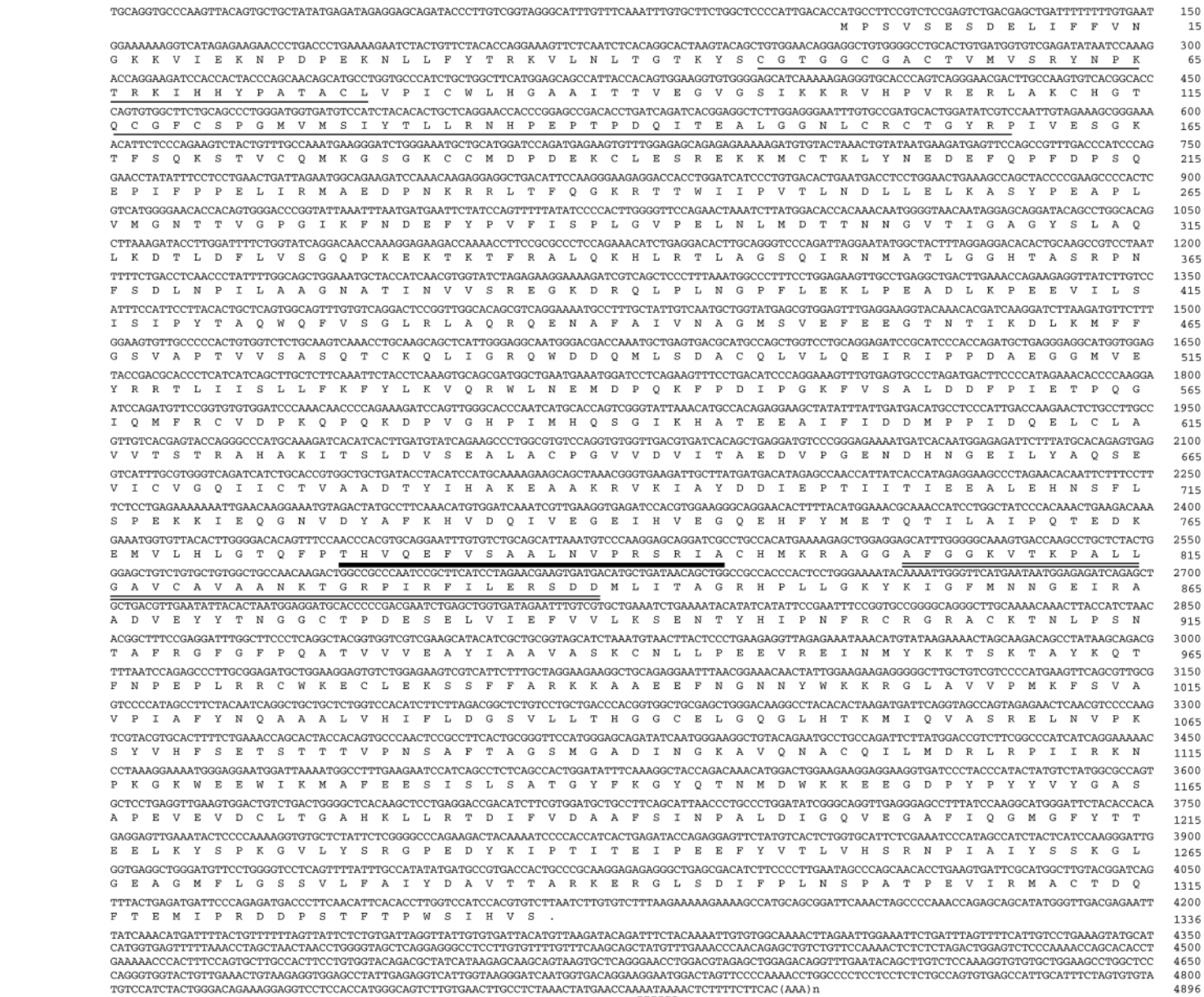

FIG. 3. **Nucleotide and deduced amino acid sequence of mouse skin AOH2.** The nucleotide sequence of the AOH2 cDNA (*upper line*) was obtained from the overlapping cDNA fragments shown in Fig. 1 and is presented with its deduced amino acid sequence (*lower line*). Nucleotides are numbered in the 5′–3′ direction, whereas amino acids are numbered from the amino terminus to the carboxyl terminus starting from the putative first methionine residue. (*AAA*)*n* indicates the polyadenylated tail of the transcript. The sequences corresponding to the 2Fe-2S redox centers are *underlined*, and the molybdo-protein fingerprint sequence is *doubly underlined*. The *dotted line* indicates the polyadenylation signal. The *thick line* indicates the peptide used to raise specific anti-AOH2 polyclonal antibodies.

consistent with that predicted on the basis of the two deduced amino acid sequences and similar to that of the monomeric subunits of AOs and XORs. The three polyclonal antibodies do not show cross-reactivity with mouse XOR as well (data not shown), demonstrating that they are mono-specific.

To study the enzymologic characteristics of AOH1 and AOH2, we evaluated whether the two proteins are able to oxidize substrates specific for AO (benzaldehyde and phenanthridine) and XOR (hypoxanthine). As illustrated in Fig. 6*B* and as already reported by Holmes (36), upon cellulose-acetate electrophoresis, two cathodic benzaldehyde-oxidizing bands (band α and β) are evident in liver extracts. Zymograms of HEK293 cell extracts transfected with pCMV, pCMV-XOR, or pCMV-AOH2 do not contain significant amounts of benzaldehyde-oxidizing activity. Interestingly, forced expression of the AOH1 and AO cDNAs results in the appearance of benzaldehyde-oxidizing bands with the same mobility as liver band α and β, respectively. As expected (36–39), transfection of the XOR construct gives rise to a slowly migrating anodic band (band γ) with strong hypoxanthine-oxidizing activity. The mobility of this band is coincident with that of intact XOR in liver extracts. In the same zymogram, the lanes corresponding to cells transfected with AOH1, AOH2, and AO are devoid of bands with hypoxanthine oxidizing activity. As documented in Fig. 6*C*, programmed expression of the AOH1 and AOH2 proteins results in a level of phenanthridine-oxidizing activity that is significantly above that observed in untransfected or pCMV-transfected HEK293 cells. This activity is of the same order of magnitude as that observed following forced expression of pCMV-AO. Association of phenanthridine oxidizing activity with AOH2 was further confirmed by transfection of pCMV-AOH2 in HC11 mouse mammary cells. In this cell line, we measured 23.9 ± 6.8, 49.2 ± 9.0, and 50.7 ± 5.3 milliunits/mg of protein (mean ± S.D. of at least two independent experi-

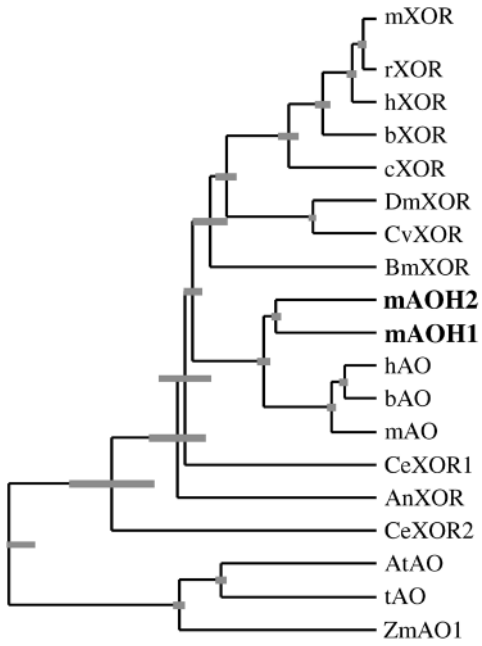

FIG. 4. **Phylogenetic tree of animal and plant molybdo-flavoenzymes.** The phylogenetic tree was constructed by computer-assisted comparison of AOH1, AOH2, and the indicated AO and XOR sequences using the Clustal algorithm contained in the GeneWork software package (Intelligenetics Inc., Palo Alto, CA). *m,* mouse; *r,* rat; *h*, human; *b*, bovine; *c*, chicken; *Dm*, *D. melanogaster*; *Cv*, *Calliphora vicina*; *Bm, B. mori*; *Ce*, *Caenorhabditis elegans*; *An*, *A. nidulans*; *At*, *A. thaliana*; *t*, tomato; *Zm, Zea maize*.

ments run in triplicate), following transfection of pCMV, pCMV-AOH2, and pCMV-AO, respectively.

In their active conformation, AO and XOR proteins are believed to be homodimers with an approximate molecular mass of 300 kDa (18, 19). Thus, we deemed it of interest to investigate the structure of the catalytically active form of AOH1. As shown in Fig. 6*D* (*inset a*), we obtained a semi-purified preparation of mouse liver molybdo-flavoproteins (containing AOH1 and AO) in their catalytically active forms (*inset b*) by affinity chromatography on benzamidine-Sepharose (13). The mixture was applied to an FPLC size exclusion column. Aliquots of the resulting chromatographic fractions were analyzed for the presence of benzaldehyde oxidizing activity by cellulose acetate electrophoresis, as well as AOH1 and AO immunoreactivity by Western blot analysis. AOH1 enzymatic activity (benzaldehyde-oxidizing band α, chromatogram) and immunoreactivity (*inset c*) reproducibly elute in the same fractions of the column with a calculated apparent molecular mass of approximately 600 kDa, which decreased to 150 kDa after denaturation and reduction (*inset c*). The same column fractions that contain AOH1 also contain AO immunoreactivity (*inset c*) and enzymatic activity (benzaldehyde oxidizing band β, data not shown). This suggests that the catalytically active forms of mouse AOH1 and AO have a similar multimeric structure, which is compatible with that of a tetramer consisting of four identical subunits of approximately 150 kDa each. At present, we do not know why, under our experimental conditions, mouse AO behaves as a homotetramer rather than a homodimer, like AOs of other origin (18, 19).

Tissue Distribution of the Mouse AOH1 and AOH2 Transcripts and Proteins—By using the AOH1 and AOH2 cDNAs as probes, the tissue distribution of the corresponding mRNAs was studied by Northern blot analysis. As documented by Fig. 7*A*, a single AOH1 mRNA species is detectable in the liver, testis, and lung, whereas all the other tissues do not synthesize detectable amounts of the transcript. The tissue distribution of AOH1 is very similar to that of mouse AO (14) but significantly different from that of the corresponding XOR mRNA (24). The AOH2 transcript levels are relatively low, being detectable only upon enrichment of the poly(A^+) fraction of cellular RNA. The expression profile of the AOH2 mRNA is entirely distinct from that of the AOH1 or AO transcripts and is restricted to the stomach, skin, esophagus, and oral cavity (not shown).

By using the specific antibodies described above, we determined the tissue distribution of the AOH1 and AOH2 proteins and compared it with that of AO. As to AOH1, the Western blot analysis presented in Fig. 7*B* demonstrates that liver, lung, and testis (visible only upon longer exposure of the film) synthesize significant amounts of the protein, confirming the results obtained at the mRNA level. The tissues that synthesize the AOH1 protein are the same in which significant amounts of the AO counterpart are observed, supporting co-expression of the relative genes. Despite comparable mRNA levels, the liver accumulates much larger amounts of the AOH1 protein than the testis, suggesting the existence of cell-specific translational and/or post-translational regulatory mechanisms. As to AOH2, synthesis of the protein is limited to the skin, stomach, and esophagus, as expected from the corresponding mRNA data. A second band of slightly higher molecular weight is observed in the esophagus and stomach. This second band is of unknown origin, although it does not represent a phosphorylated or glycosylated form of AOH2 (data not shown). As shown in Fig. 7*C*, by far the highest levels of benzaldehyde-oxidizing activity are present in the liver, although detectable amounts of band α and band β are evident also in the lung. Significantly and as expected on the basis of the lack of benzaldehyde oxidizing activity associated with AOH2 (see Fig. 6*B*), the zymogram of skin extracts is devoid of protein bands that can be stained upon incubation with benzaldehyde as a substrate.

Holmes (36, 39) reported that the two liver benzaldehyde-oxidizing isoenzymes corresponding to bands α and β are present in higher amounts in the male than in the female organ. This is confirmed by the zymogram shown in Fig. 7*C*. In line with the concept that AOH1 and AO are responsible for the enzymatic activities associated with bands α and β, respectively, Fig. 7*D* (*right panel*) demonstrates that both the AOH1 and AO immunoreactive bands are present in larger amounts in male than in female livers. Gender-associated differences in the amounts of AOH1 and AO proteins are not observed in the lung and other organs (data not shown), demonstrating that the phenomenon is liver-specific. As previously noticed in the case of AO (14), higher levels of AOH1 protein in male than in female hepatocytes are associated with equal amounts of the corresponding transcripts in the two genders (Fig. 7*D, left panel*). In liver, *AOH1* is the first gene to be turned on during ontogeny. In fact, as shown in Fig. 7*E*, whereas the newborn contains amounts of the AOH1 transcript that are comparable to those observed in the adult animal, significant levels of the AO mRNA are present only during adulthood. The AOH1 protein is already observed in the 18-day-old embryo, although synthesis of the polypeptide is significantly elevated soon after birth and reaches its peak only after maturation of the mouse. By contrast, the AO immunoreactive band is visible only in the adult mouse. Cellulose acetate electrophoresis demonstrates that only benzaldehyde-oxidizing band α is expressed in the newborn and 5-day-old animal. This further strengthens the argument that band α is due to AOH1 and band β corresponds to AO.

Identification of Cells Expressing AOH1 and AOH2 in Mouse Tissues—To identify the type of cells responsible for the synthesis of the mouse AOH1 and AOH2 transcripts, *in situ* hybridization experiments were performed. As illustrated in Fig.

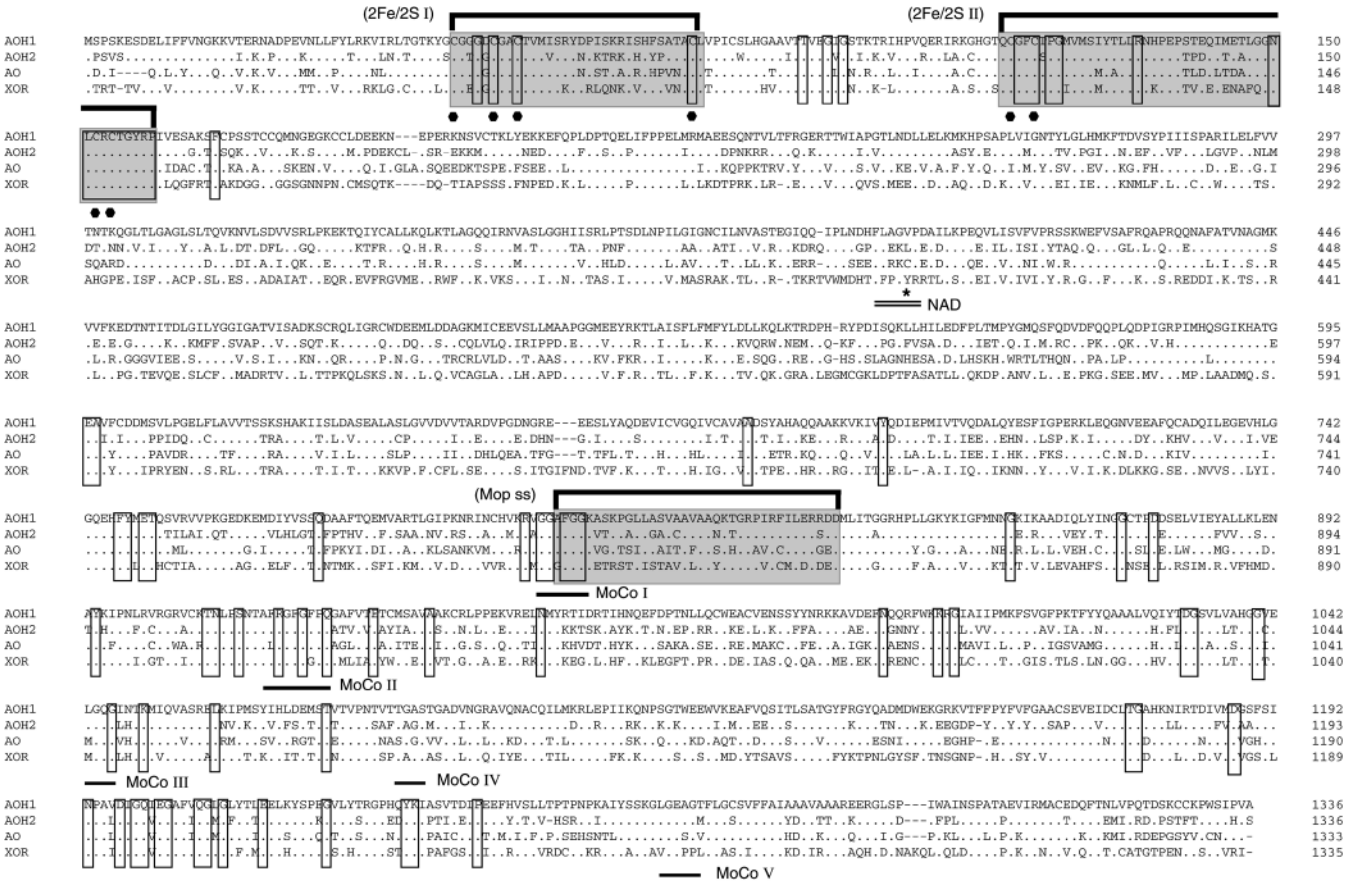

FIG. 5. **Amino acid sequence comparison among mouse AOH1, AOH2, AO, and XOR.** The amino acid sequence of mouse AOH1 is aligned with that of AOH2, AO, and XOR. Amino acid residues are numbered from the amino terminus to the carboxyl terminus from the putative first methionine of each sequence. *Dots* indicate identical amino acids relative to the AOH1 sequence. *Hyphens* represent gaps introduced to obtain the best alignment. Residues conserved in AOH1, AOH2, and all the AO and XOR sequences so far identified are *boxed*. The Cys residues reported to be involved in the formation of the iron-sulfur centers are indicated by *solid hexagons below* the sequences. The sequence of mouse XOR corresponding to the putative NAD^+-binding site (NAD), experimentally determined for chicken XOR (55), is *doubly underlined* at the *bottom* of the sequences, and the photolabeled tyrosine residue is indicated by an *asterisk*. The consensus sequence pattern for the molybdopterin cofactor-binding site and the 2Fe-2S redox centers are indicated by *thick solid lines above* the sequences and *shaded boxes* (Mop SS, *molybdo-protein s*ignature sequence; 2Fe/2S I and 2Fe/2S II). The MoCoI-MoCoV sequences are indicated by *thick lines below* the sequences. Computer-assisted alignment of the various sequences was performed with the Clustal algorithm used in the Genwork software package (Intelligenetics, Mountain View, CA).

8*A*, when the AOH1 antisense cRNA is used as a probe, accumulation of silver grains is selectively observed in the hepatocytic component of the liver of adult mice. The use of the corresponding sense cRNA as a negative control does not result in the appearance of a significant number of silver grains on adjacent tissue slides (Fig. 8*B*). These results demonstrate that the hepatocyte is the only cell type that synthesizes significant amounts of the AOH1 transcript in the liver of the adult animal. We noticed a steep gradient in the expression of the *AOH1* gene, as we proceed from the periportal to the perivascular region of the hepatocytic trabeculae. In the testis, expression of AOH1 is selectively observed in the spermatogonia, which are localized inside the seminiferous tubules in close juxtaposition with mature spermatozoa (Fig. 8*C*).

In the case of AOH2, expression is limited to the epithelial component of squamous tissues. As shown in Fig. 9*A*, in the oral cavity, the cells contained in the multilayered and highly keratinized epithelium of the papillae of the tongue can be easily marked with a radioactive AOH2 antisense but not with the corresponding sense cRNA probe (Fig. 9, *A* and *B*). The squamous epithelium of the esophagus (Fig. 9, *C* and *D*) and the proximal portion of the stomach (Fig. 9, *E* and *F*) as well as the epidermis (Fig. 9, *G* and *H*) are also rich sources of AOH2-expressing cells. In all these squamous epithelia, AOH2 is synthesized predominantly in the basal proliferating compartment of cells which are bound to undergo the process of keratinization and involution observed in the most superficial layer. In the epidermis, a very high level of AOH2 mRNA accumulation is also evident in the epithelial cells representing the bulbar portion of the hair folliculi (data not shown). Only background accumulation of silver grains is observed in the mesenchymal and muscular cells of the tongue, esophagus, and stomach, as well as in the dermal and subdermal layer of the skin. The AOH2 transcript is not expressed in the mucosal and non-keratinized portions of the stomach (fundus and pylorus; data not shown).

DISCUSSION

In this article, we report on the isolation and characterization of two novel members of the molybdo-protein family, AOH1 and AOH2. The cDNAs coding for both AOH1 and AOH2 were cloned because of their striking resemblance with the molybdo-flavoproteins AO and XOR. This is the first indication that the family of mammalian molybdo-proteins extends beyond sulfite oxidase, AO and XOR. In fact, although we did not directly demonstrate the presence of a molybdenum cofactor associated with the two polypeptides, AOH1 and AOH2 are almost certainly molybdo-enzymes because they contain the fingerprint sequence observed in all prokaryotic and eukaryotic molybdo-proteins. In addition, they show conservation in 3 out

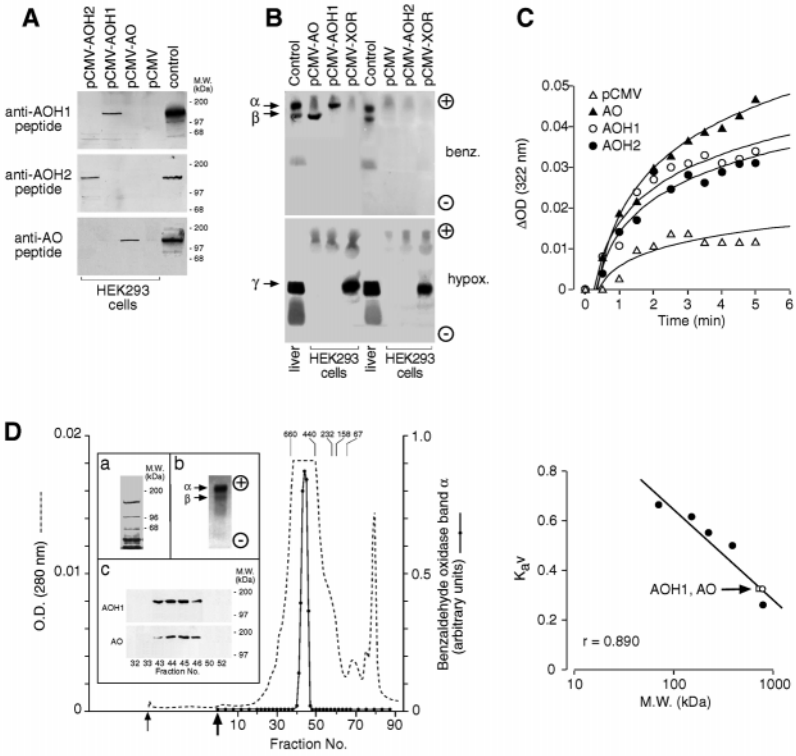

FIG. 6. **Biochemical and immunological characterization of the AOH1 and AOH2 proteins.** *A,* immunoreactivity of AOH1, AOH2, and AO proteins. Extracts from transfected HEK293 (100 μg of protein) were subjected to Western blot analysis using rabbit polyclonal antibodies raised against synthetic peptides derived from the amino acid sequences of AOH1, AOH2, and AO. The position of the molecular mass markers is indicated on the *right* (200 kDa, myosin heavy chain; 97 kDa, phosphorylase *b*; 68 kDa, bovine serum albumin). Liver (AOH1 and AO) and skin (AOH2) extracts were used in control lanes. *B,* cellulose acetate zymograms of HEK293 cells transfected with the AOH1, AOH2, AO, and XOR cDNAs. HEK293 fibroblasts (2×10^6 cells were plated 24 h before transfection) were transiently transfected with constructs (16 μg/plate) allowing expression of the AOH1 (pCMV-AOH1), the AOH2 (pCMV-AOH2), the AO (pCMV-AO), and the XOR (pCMV-XOR) proteins or with vector alone (pCMV). Forty eight hours following transfection, an equivalent amount of cell extracts (150 μg of protein) was subjected to electrophoresis on cellulose acetate plates. Plates were developed to reveal aldehyde or xanthine oxidase enzymatic activities using benzaldehyde (*benz.*) or hypoxanthine (*hypox.*) as substrates and PMS and MTT as electron acceptors. Following development of the purple stains corresponding to the aldehyde (α and β bands) or xanthine (γ band) oxidase activities, plates were photographed. Liver cytosolic extracts were used as positive controls for the staining procedure (*control*). *C,* phenanthridine oxidizing activity of HEK293 cells transfected with the AOH1, AOH2, AO, and XOR cDNAs. Protein extracts (100 μg) from transfected HEK293 prepared as in *A* were incubated at room temperature for the indicated amount of time with phenanthridine as a substrate. Oxidation of phenanthridine to 6-phenanthridone was evaluated spectrophotometrically by continuously measuring the increase in absorbance (ΔOD) at 322 nm. *D,* apparent molecular weight of the catalytically active form of AOH1. The mouse AOH1 and AO enzymes were partially purified by benzamidine-Sepharose affinity chromatography. A Coomassie Blue staining of an SDS-PAGE of the semi-purified protein preparation (*inset a*) is shown along with a cellulose acetate zymogram developed with benzaldehyde as the substrate (*inset b*). The benzamidine-Sepharose eluate was subjected to gel permeation chromatography on a Superose 6 FPLC column calibrated with proteins of known molecular weight (thyroglobulin, 660 kDa; ferritin, 440 kDa; catalase, 232 kDa; aldolase, 158 kDa; albumin, 67 kDa). Aliquots of the collected fractions were subjected to enzymatic and Western blot analyses. The elution profile of the AOH1 enzymatic activity (benzaldehyde-oxidizing band α) is indicated by the *solid line* of the chromatogram and was obtained by densitometric analysis (*right ordinate axis*) of the zymogram of each column fraction. The *dashed line* indicates the elution profile of proteins as assessed by determination of the absorbance at 280 nm (*left ordinate axis*). The *thin arrow* indicates injection of the sample, and the *thick arrow* indicates start of fraction collection. Western blot analyses of the chromatographic fractions using anti-AOH1 and anti-AO polyclonal antibodies are shown in *inset c* (only peak fractions and appropriate negative fractions are presented). The right portion of *D* shows the calibration curve of molecular weight standards along with the extrapolated apparent molecular weight of the AOH1 and AO proteins. $K_{av} = V_e - V_0/V_t - V_0$, where V_e is the elution volume for the protein, V_0 is the column void volume, and V_t is the total bed volume. All the experiments presented are representative of at least three others, giving essentially the same results.

of the 5 sequences, MoCoI–MoCoV, present in DvgAOX (53) and conserved in XORs and AOs (3–5, 8–10, 12–14, 34, 45–49). The remarkable resemblance of AOH1 and AOH2 to AO and XOR suggests that the two proteins are not only molybdo- but they are also flavoenzymes. Consistent with this, the two novel proteins share a relatively conserved region upstream of the molybdenum site, where the as yet unidentified FAD binding domain of XOR and AO is believed to reside (1). The similarity among AOH1, AOH2, AO, and XOR extends to the general structural architecture of the four proteins. In fact, both AOH1 and AOH2 contain amino-terminal domains that have strong similarity with the two non-identical 2Fe/2S centers typical of all the AO and XOR proteins. In addition, the multimeric structure of the catalytically active form of AOH1 is the same as that of mouse AO.

The two novel proteins AOH1 and AOH2 are more similar to AO than to XOR. In particular, the lack of an NAD-binding site conserved in all XORs and the absence of a Glu residue (aa 805 of mouse XOR), which plays a critical role in binding the imino function of xanthine, support the idea that AOH1 and AOH2 are oxidases acting on substrates different from those of XOR. In line with this, recombinant AOH1 and AOH2 oxidize phenanthridine, a relatively specific substrate of AO, whereas they are incapable of oxidizing hypoxanthine, which represents a selective XOR substrate. In addition, AOH1, but not AOH2, oxidizes benzaldehyde. With respect to this, AOH1 and AO have the same characteristics as the liver benzaldehyde oxidizing activities reported by Holmes (36) to be the products of two genetic loci, named *AOX1* and *AOX2*. Furthermore, that AOH1 and AO are indeed the products of the *AOX1* and *AOX2* loci,

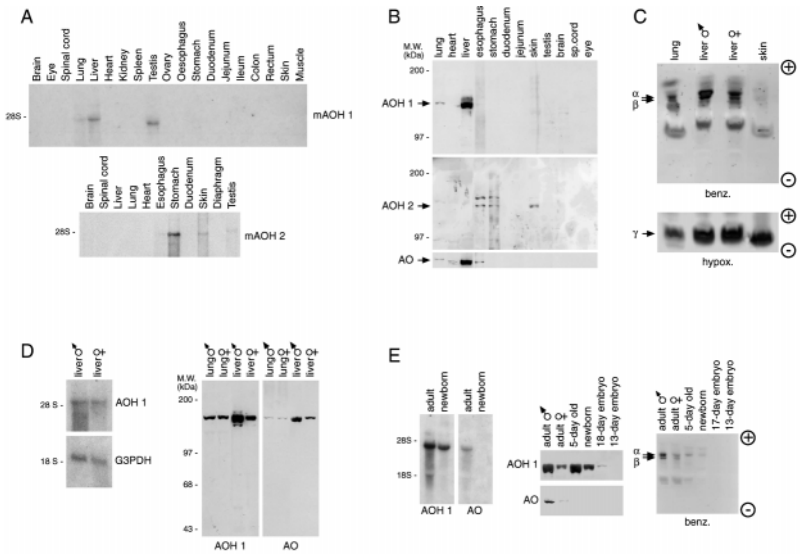

FIG. 7. **Tissue distribution, sex-related differences, and ontogeny of AOH1 and AOH2 mRNAs and proteins.** *A,* tissue distribution of the AOH1 and AOH2 transcripts. Total RNA (*upper panel*) or poly(A$^+$) RNA (*lower panel*) was obtained from the indicated tissues. RNA (20 μg/lane) was loaded on a 1% formaldehyde/agarose gel and subjected to Northern blot analysis. After transfer, nylon membranes were hybridized with the mouse AOH1 and AOH2 full-length cDNAs. The positions of 28 S and 18 S rRNA are shown on the *left. B,* tissue distribution of the AOH1, AOH2, and AO proteins. Extracts from the indicated tissues (100 μg of protein/lane) were loaded on 6% polyacrylamide slab gels, transferred to nitrocellulose membranes, and subjected to Western blot analysis with anti-AOH1 (*upper panel*), anti-AOH2 (*middle panel*), and anti-AO antibodies (*lower panel*). The position of molecular mass standards is indicated on the *left* (200 kDa, myosin heavy chain; 97 kDa, phosphorylase *b*). *C,* benzaldehyde oxidase and xanthine oxidase zymograms of tissue extracts. Protein extracts (150 μg/lane) from the indicated tissues were loaded in the middle of cellulose acetate plates and electrophoresed. Plates were developed for benzaldehyde oxidase (*benz.*) or hypoxanthine oxidase (*hypox.*) activity by overlaying a 1% agarose solution containing PMS, MTT, and benzaldehyde or hypoxanthine. The direction of migration from the anode (−) to the cathode (+) is indicated on the *right. D,* gender-specific accumulation of AOH1 and AO transcripts (*left panel*) and proteins (*right panel*) in liver. Protein extracts from liver and lung of three female and male animals were pooled, and aliquots (100 μg of protein/lane) were subjected to Western blot analysis with anti-AOH1 and anti-AO antibodies as indicated. The position of the molecular weight standards is indicated on the left (200 kDa, myosin heavy chain; 97 kDa, phosphorylase *b*; 68 kDa, bovine serum albumin; 43 kDa, ovalbumin). *E,* ontogeny of AOH1 and AO transcripts, protein and enzymatic activity. *Left panel,* total RNA was extracted from livers of 3 newborn and 3 adult animals and subjected to Northern blot analysis using specific AOH1 and AO cDNA probes as indicated. *Middle panel,* extracts from livers obtained from fetuses at different gestational age, from newborn or from adult animals, as indicated, were subjected to Western blot analysis using anti-AOH1 and anti-AO antibodies. *Right panel,* extracts from the indicated tissues were electrophoresed on cellulose acetate plates. Plates were developed for benzaldehyde oxidase (*benz.*) enzymatic activity, as in *C*.

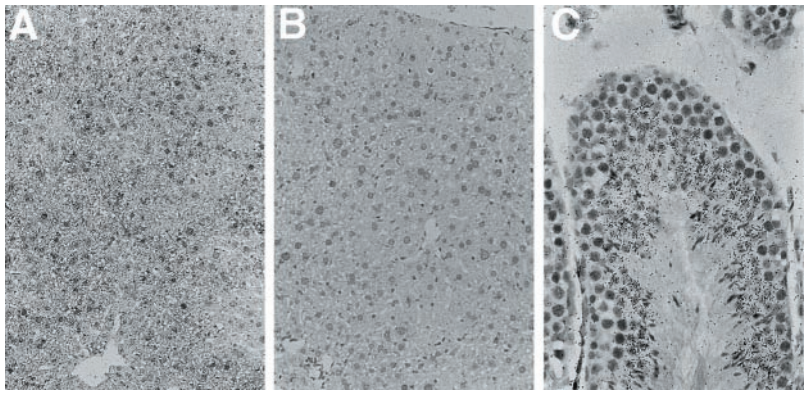

FIG. 8. ***In situ* hybridization of the AOH1 transcript in liver and testis.** Tissue sections derived from mouse liver (*A* and *B*) and testis (*C*) were hybridized with a ^{35}S-radiolabeled AOH1 antisense cRNA (*A* and *C*) or the corresponding sense cRNA (*B*). The magnification of the light field photographs of *A* and *B* is × 200 and that of *C* is × 400.

respectively, is supported by the ontogeny and the gender-specific regulation of the two proteins. In addition, along with *AOH2*, the *AOH1* and *AO* genes cluster on chromosome 1 at a short distance from each other,[2] consistent with Holmés data (36) for the *AOX1* and *AOX2* loci. Finally, the structural organization of the *AOH1* and *AOH2* genes is very similar to that of AO (22).[2] Thus, we propose that AOH1, AOH2, and AO are all aldehyde oxidase isoenzymes acting on different but overlapping sets of substrates.

The tissue and cell distribution of AOH1 and AOH2 is very different and suggests distinct physiological functions for the two proteins. AOH1 is synthesized in the hepatocyte, in the lung, and the testis. In the liver, the synthesis of the AOH1 protein is likely to be under the control of male sex hormones, since the enzyme is present in the male hepatocyte in much larger amounts than in the female counterpart. The tissue distribution and the gender-specific regulation of AOH1 is strikingly similar to that of AO, suggesting remarkable co-regulation. So far, the only observed difference in the pattern of expression between the two enzymes is during development. In fact, the *AOH1* gene is expressed in the liver of fetuses and newborn animals, whereas the *AO* counterpart is switched on only during adulthood. All this suggests that AOH1 and AO serve similar or complementary physiological function and they may have distinct roles during the development of the male organism. Significantly, both AOH1 and AO proteins are synthesized in the male but not in the female reproductive organ. This indicates that the two enzymes may be involved in the

[2] E. Garattini and M. Terao, manuscript in preparation.

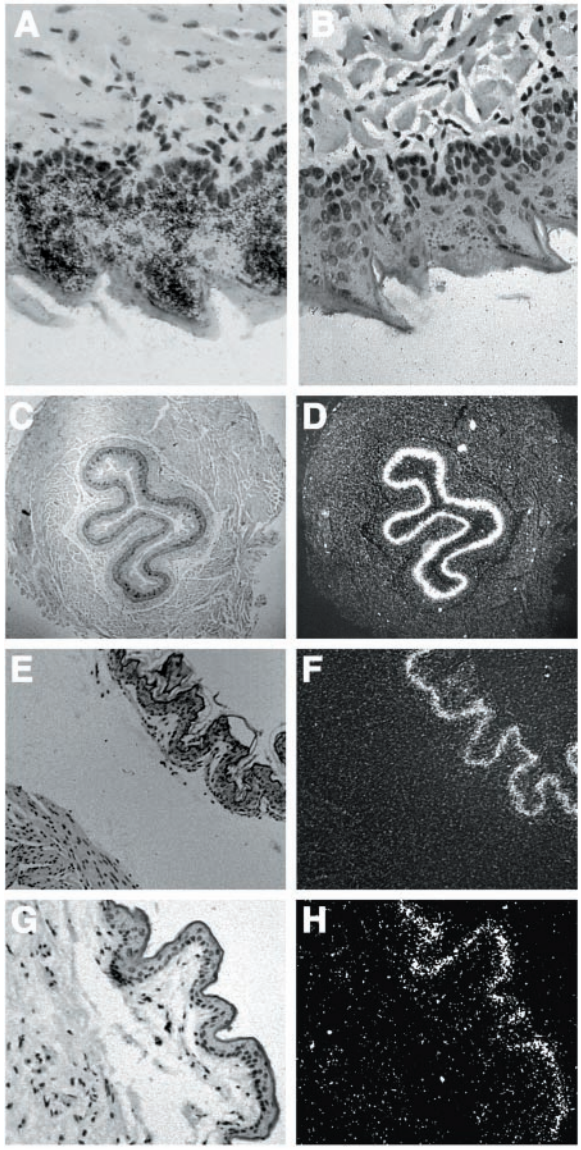

FIG. 9. ***In situ* hybridization of the AOH2 transcript in the tongue, esophagus, stomach, and skin.** Tissue sections derived from mouse tongue (*A* and *B*), esophagus (*C* and *D*), proximal portion of the stomach (*E* and *F*), and foreskin (*G* and *H*) were hybridized with a ^{35}S-radiolabeled AOH2 antisense cRNA (*A* and *C–H*) or the corresponding sense cRNA (*B*). Light field (*A, C, E* and *G*) and dark field (*D, F,* and *H*) micrographs are shown. The magnification of photographs in *A* and *B* is × 400, in *C* and *D* is × 40, and in *E–H* is × 200.

process of maturation of germinal cells in the testis and suggests that the physiological substrate(s) of AOH1 and AO may be sought for among the metabolites of the sex steroid hormone pathway.

The tissue and cell distribution of AOH2 is much more restricted than that of AOH1. In fact, expression is limited to the epithelial component of the mouse squamous mucosae and skin. In the skin, AOH2 seems to be synthesized during the first phases of the keratinocyte differentiation program, as large amounts of the transcript are located in the basal layer of the epidermis and in the bulbar portion of the hair folliculi. Consistent with this, AOH2 mRNA levels increase when the MK mouse keratinocyte cell line is induced to mature along the keratinocyte pathway following calcium withdrawal from the culture medium.[3] Thus, it is possible that AOH2 plays a role in the process of homeostasis and/or differentiation of the keratinocyte and the squamous epithelial cell in more general terms. With respect to this, it could be speculated that, as already suggested for AO (32), AOH2 also has a role in the metabolism of natural retinoids, which are well known determinants of the differentiation state of the keratinocyte (56).

In conclusion, the identification of two novel members of the mammalian molybdo-flavoprotein family has already brought novel information as to the structure, the function, and the phylogenesis of this class of enzymes. We are currently in the process of assessing whether human orthologs of mouse AOH1 and AOH2 exist by cloning the respective cDNAs and genes. The existence of human counterparts for the AOH1 and AOH2 proteins would have profound implications for the etiology and pathogenesis of rare hereditary diseases known to or purported to involve molybdo-proteins, such as the combined deficiency of the molybdenum cofactor (57) and the recessive familial form of amyotrophic lateral sclerosis (50).

Acknowledgments—We are grateful to Prof. Silvio Garattini for useful suggestions and critical reading of the manuscript.

[3] E. Garattini and M. Terao, unpublished results.

REFERENCES

1. Hille, R. (1996) *Chem. Rev.* **96,** 2757–2816
2. Rebelo, J., Macieira, S., Dias, J. M., Huber, R., Ascenso, C. S., Rusnak, F., Moura, J. J., Moura, I., and Romao, M. J. (2000) *J. Mol. Biol.* **297,** 135–146
3. Glatigny, A., and Scazzocchio, C. (1995) *J. Biol. Chem.* **270,** 3534–3550
4. Sekimoto, H., Seo, M., Dohmae, N., Takio, K., Kamiya, Y., and Koshiba, T. (1997) *J. Biol. Chem.* **272,** 15280–15285
5. Ori, N., Eshed, Y., Pinto, P., Paran, I., Zamir, D., and Fluhr, R. (1997) *J. Biol. Chem.* **272,** 1019–1025
6. Wright, R. M., Clayton, D. A., Riley, M. G., McManaman, J. L., and Repine, J. E. (1999) *J. Biol. Chem.* **274,** 3878–3886
7. Garrett, R. M., Bellissimo, D. B., and Rajagopalan, K. V. (1995) *Biochim. Biophys. Acta* **126,** 147–149
8. Terao, M., Cazzaniga, G., Ghezzi, P., Bianchi, M., Falciani, F., Perani, P., and Garattini, E. (1992) *Biochem. J.* **283,** 863–870
9. Amaya, Y., Yamazaki, K., Sato, M., Noda, K., and Nishino, T. (1990) *J. Biol. Chem.* **265,** 14170–14175
10. Terao, M., Kurosaki, M., Zanotta, S., and Garattini, E. (1997) *Biochem. Soc. Trans.* **25,** 791–796
11. Berglund, L., Rasmussen, J. T., Andersen, M. D., Rasmussen, M. S., and Petersen, T. E. (1996) *J. Dairy Sci.* **79,** 198–204
12. Saksela, M., and Raivio, K. (1996) *Biochem. J.* **315,** 235–239
13. Li-Calzi, M., Raviolo, C., Ghibaudi, E., de Gioia, L., Salmona, M., Cazzaniga, G., Kurosaki, M., Terao, M., and Garattini, E. (1995) *J. Biol. Chem.* **270,** 31037–31045
14. Kurosaki, M., Demontis, S., Garattini, E., and Terao, M. (1999) *Biochem. J.* **341,** 71–80
15. Huang, D. Y., Furukawa, A., and Ichikawa, Y. (1999) *Arch. Biochem. Biophys.* **364,** 264–272
16. Wright, R. M., Vaitaitis, G. M., Wilson, C. M., Repine, T. B., Terada, L. S., and Repine, J. E. (1993) *Proc. Natl. Acad. Sci. U. S. A.* **90,** 10690–10694
17. Krenitsky, T. A., Neil, S. M., Elion, G. B., and Hitchings, G. H. (1972) *Arch. Biochem. Biophys.* **150,** 585–599
18. Carpani, G., Racchi, M., Ghezzi, P., Terao, M., and Garattini, E. (1990) *Arch. Biochem. Biophys.* **279,** 237–241
19. Yoshihara, S., and Tatsumi, K. (1985) *Arch. Biochem. Biophys.* **242,** 213–224
20. Cazzaniga, G., Terao, M., Lo Schiavo, P., Galbiati, F., Segalla, F., Seldin, M. F., and Garattini, E. (1994) *Genomics* **23,** 390–402
21. Terao, M., Kurosaki, M., Demontis, S., Zanotta, S., and Garattini, E. (1998) *Biochem. J.* **332,** 383–393
22. Demontis, S., Kurosaki, M., Saccone, S., Motta, S. Garattini, E., and Terao, M. (1999) *Biochim. Biophys. Acta* **1489,** 207–222
23. Kurosaki, M., Zanotta, S., Li Calzi, M., Garattini, E., and Terao, M. (1996) *Biochem. J.* **319,** 801–810
24. Kurosaki, M., Li Calzi, M., Scanziani, E., Garattini, E., and Terao, M. (1995) *Biochem. J.* **306,** 225–234
25. Fridovich, I. (1970) *J. Biol. Chem.* **245,** 4053–4057
26. Parks, D. A., and Granger, D. N. (1983) *Am. J. Physiol.* **245,** G285–G289
27. Page, S., Powell, D., Benboubetra, M., Stevens, C. R., Blake, D. R., Selase, F., Wolstenholme, A. J., and Harrison, R. (1998) *Biochim. Biophys. Acta* **1381,** 191–202
28. Akaike, T., Ando, M., Oda, T., Doi, T., Ijiri, S., Araki, S., and Maeda, H. (1990) *J. Clin. Invest.* **85,** 739–745
29. Huang, D. Y., and Ichikawa, Y. (1994) *Biochem. Biophys. Res. Commun.* **205,** 1278–1283
30. McGeer, E. J., and McGeer, P. L. (eds) (1978) *Molecular Neurobiology of Mammalian Brain,* Plenum Publishing Corp., New York
31. Fabre, G., Seither, R., and Goldman, I. D. (1986) *Biochem. Pharmacol.* **35,** 1325–1330
32. Cates, L. A., Jones, G. S., Jr., Good, D. J., Tsai, H. Y., Li, V. S., Caron, N., Tu, S. C., and Kimball, A. P. (1980) *J. Med. Chem.* **23,** 300–304
33. Berger, R., Mezey, E., Clancy, K. P., Harta, G., Wright, R. M., Repine, J. E., Brown, R. H., Brownstein, M., and Patterson, D. (1995) *Somatic Cell Mol.*

Genet. **21,** 121–131
34. Sekimoto, H., Seo, M., Kawakami, N., Komano, T., Desloire, S., Liotenberg, S., Marion-Poll, A., Caboche, M., Kamiya, Y., and Koshiba, T. (1998) *Plant Cell Physiol.* **39,** 433–442
35. Wright, R. M., and Repine, J. E. (1997) *Biochem. Soc. Trans.* **25,** 799–804
36. Holmes, R. S. (1979) *Biochem. Genet.* **17,** 517–528
37. Maniatis, T., Fritsch, E. F., and Sambrook, J. (eds) (1989) *Molecular Cloning: A Laboratory Manual*, Cold Spring Harbor Laboratory, Cold Spring Harbor, NY
38. Sanger, F., Nicklen, S., and Coulson, A. R. (1977) *Proc. Natl. Acad. Sci. U. S. A.* **74,** 5463–5467
39. Holmes, R. S. (1978) *Comp. Biochem. Physiol. B Comp. Biochem. Mol. Biol.* **61,** 339–347
40. Taylor, S. M., Stubley-Beedham, C., and Stell, J. G. P. (1984) *Biochem. J.* **220,** 67–74
41. Tam, J. P. (1988) *Proc. Natl. Acad. Sci. U. S. A.* **85,** 5409–5414
42. Persico, M. G., Viglietto, G., Martini, G., Toniolo, D., Paonessa, G., Moscatelli, C., Dono, R., Vulliamy, T., Luzzatto, L., and D'Urso, M. (1986) *Nucleic Acids Res.* **14,** 2511–2520
43. Angerer, L. M., and Angerer, R. C. (1992) in *In Situ Hybridization: A Practical Approach* (Wilkinson, D. G., ed) pp. 15–32, IRL Press at Oxford University Press, Oxford
44. Hofmann, K., Bucher, P., Falquet, L., and Bairoch, A. (1999) *Nucleic Acids Res.* **27,** 215–219
45. Keith, T. P., Riley, M. A., Kreitman, M., Lewontin, R. C., Curtis, D., and Chambers, G. (1987) *Genetics* **116,** 67–73
46. Yasukochi, Y., Kanda, T., and Tamura, T. (1998) *Genet. Res.* **71,** 11–19
47. Sato, A., Nishino, T., Noda, K., Amaya, Y., and Nishino, T. (1995) *J. Biol. Chem.* **270,** 2818–2826
48. Houde, M., Tiveron, M. C., and Bregegere, F. (1989) *Gene* (*Amst.*) **85,** 391–402
49. The *Caenorhabditis elegans* Sequencing Consortium (1998) *Science* **282,** 2012–2018
50. Hosler, B. A., Sapp, P. C., Berger, R., O'Neill, G., Bejaoui, K., Hamida, M. B., Hentati, F., Chin, W., McKenna-Yasek, D., Haines, J. L., Patterson, D., Horvitz, H. R., Brown, R. H., Jr., and Day, C. B. (1998) *Neurogenetics* **2,** 34–42
51. Correll, C. C., Ludwig, M. L., Bruns, C. M., and Karplus, P. A. (1993) *Protein Sci.* **2,** 2112–2133
52. Thoenes, U., Flores, O. L., Neves, A., Devreese, B., Van Beeumen, J. J., Huber, R., Romao, M. J., LeGall, J., Moura, J. J., and Rodrigues-Pousada, C. (1994) *Eur. J. Biochem.* **220,** 901–910
53. Romao, M. J., Archer, M., Moura, I., Moura, J. J. G., LeGall, J., Engh, R., Schneider, M., Hof. P., and Huber, R. (1995) *Science* **270,** 1170–1176
54. Glatigny, A., Hof, P., Romao, M. J., Huber, R., and Scazzocchio, C. (1998) *J. Mol. Biol.* **278,** 431–438
55. Nishino, T., and Nishino, T. (1989) *J. Biol. Chem.* **264,** 5468–5473
56. Sasai, Y., and De Robertis, E. M. (1997) *Dev. Biol.* **182,** 5–20
57. Reiss, J. (2000) *Hum. Genet.* **106,** 157–163

Cloning of the cDNAs Coding for Two Novel Molybdo-flavoproteins Showing High Similarity with Aldehyde Oxidase and Xanthine Oxidoreductase

Mineko Terao, Mami Kurosaki, Giuliana Saltini, Silvia Demontis, Massimiliano Marini, Mario Salmona and Enrico Garattini

J. Biol. Chem. 2000, 275:30690-30700.
doi: 10.1074/jbc.M005355200 originally published online July 11, 2000
